The *Caenorhabditis elegans* vulval morphogenesis gene *sqv-4* encodes a UDP-glucose dehydrogenase that is temporally and spatially regulated

Ho-Yon Hwang and H. Robert Horvitz*

Howard Hughes Medical Institute, Department of Biology, 68-425, Massachusetts Institute of Technology, Cambridge, MA 02139

Contributed by H. Robert Horvitz, August 27, 2002

The development of the *Caenorhabditis elegans* vulva requires the involution of epithelial cells and provides a model for organ morphogenesis. Mutations in *C. elegans sqv* (squashed vulva) genes affect both vulval morphogenesis and embryonic development. We found that *sqv-4* encodes a protein similar to UDP-glucose dehydrogenases and showed that the SQV-4 protein specifically catalyzes the conversion of UDP-glucose to UDP-glucuronic acid, which is essential for the biosynthesis of chondroitin and heparan sulfate proteoglycans. SQV-4 is expressed in the vulva and in oocytes, among many other cells, and SQV-4 levels are dramatically increased in a specific subset of vulval cells during vulval morphogenesis. We propose that the regulation of UDP-glucuronic acid production in a specific subset of vulval cells helps determine the shape of the vulva.

The significance of glycosaminoglycans (GAGs) in animal development has become evident in the past few years from studies of mutants defective in GAG biosynthesis. For example, the genes *sqv-1*, *-3*, *-7*, and *-8* (*sq*uashed *v*ulva) of *Caenorhabditis elegans* have been implicated in the biosynthesis of GAGs, based on amino acid sequence similarity between their protein products and known GAG biosynthesis enzymes and on biochemical assays (1–4). In the accompanying paper (4), we show that SQV-1 is a UDP-glucuronic acid decarboxylase and synthesizes UDP-xylose from UDP-glucuronic acid. SQV-7 translocates UDP-glucuronic acid, UDP-galactose, and UDP-*N*-acetylgalactosamine from the cytoplasm to the lumen of the Golgi apparatus (1, 3). SQV-3 and SQV-8 are glycosyltransferases that likely act in the lumen of the Golgi apparatus and use UDP-galactose and UDP-glucuronic acid to build the protein core-GAG-linker region of proteoglycans (1, 2, 5).

Mutations in the human GAG galactosyltransferase I, the human *sqv-3* ortholog, are implicated as the cause of a progeroid variant of the connective-tissue disorder Ehlers-Danlos syndrome (6, 7), a group of heritable disorders characterized by hyperelasticity of the skin and hypermobile joints. Mutations in the human EXT family of genes, which encode heparan sulfate polymerases that act in heparan sulfate GAG biosynthesis, are associated with hereditary multiple exostoses, a genetic disorder characterized by many cartilaginous outgrowths (reviewed in ref. 8).

Mutations in the mammalian EXT gene family and GAG galactosyltransferase I, as well as mutations in the *C. elegans sqv-1*, *-3*, *-7*, and *-8* genes, are all expected to cause defects in the formation or modification of chondroitin and/or heparan sulfate GAGs. Chondroitin and heparan sulfate share the structure: (serine residue in the protein core)-xylose-galactose-galactose-glucuronic acid-(X-glucuronic acid)$_n$, where X is *N*-acetylgalactosamine in chondroitin and is *N*-acetylglucosamine in heparan sulfate. The four sugar chain xylose-galactose-galactose-glucuronic acid is referred to as the protein core-GAG linker region and is essential for the biosynthesis of GAGs (reviewed in ref. 9).

Mutations in the eight *sqv* genes in *C. elegans* cause defects in vulval morphogenesis and embryonic development (10). The *sqv* mutants are reduced in the separation between the anterior and posterior halves of the vulva in the L4 larval stage (Fig. 1). Stronger mutant alleles of the *sqv* genes cause the maternal-effect lethal (Mel) phenotype with arrests in embryonic and larval development. In this manuscript, we report the molecular characterization of *sqv-4*. We show that *sqv-4* encodes a protein similar to UDP-glucose dehydrogenases and demonstrate that recombinant SQV-4 synthesizes UDP-glucuronic acid, which is essential for the biosynthesis of GAGs. We find dynamic temporal and cell-specific regulation of SQV-4 expression in a specific subset of vulval cells during vulval morphogenesis.

Materials and Methods

Genetics. *C. elegans* was cultured at 20–22°C as described by Brenner (11). N2 was the standard WT strain (11). Mutations used are described by Riddle *et al.* (12) unless otherwise noted. The following mutations were used: linkage group (LG)I, *lin-11(n389)*; LGIII, *lin-12(n137)*; LGV, *unc-42(e270)*, *sDf35* (13), *sqv-4(n2827, n2840)*, *emo-1(oz1)*, and *nT1(n754)* (14).

Molecular Biology. Standard molecular biological techniques were used (15). The sequences of all amplified DNAs were determined to ensure the absence of unintended mutations. Oligonucleotides used for amplification or mutagenesis of DNA will be provided on request.

Rescue. We injected genomic DNA into *unc-42(e270) sqv-4(n2827)/emo-1(oz1)* animals at concentrations of 3–7 μg/ml with the dominant roller marker pRF4, as described by Mello *et al.* (16) for germline rescue. Rol lines were established, and Unc Rol animals were examined for rescue of the *sqv-4* mutant phenotype.

***sqv-4* cDNA.** A *sqv-4* cDNA was isolated from an embryonic library (17) and was found to contain an ORF identical to F29F11.1 and predicted to encode a protein of 481 aa. The F29F11.1 ORF was cloned into pPD49.78 and pPD49.83 (from A. Fire, Carnegie Institution of Washington, Baltimore), which are designed to express the transcriptionally fused ORF under the control of the *C. elegans* heat-shock promoters (18). We injected *sqv-4(n2827)/nT1(n754)* animals with these vectors along with pRF4, and Rol lines were established. Rol non-Unc animals were examined for rescue of the *sqv-4* mutant phenotype after induction of *sqv-4* expression by 30 min of heat-shock treatment at 33°C.

UDP-Glucose Dehydrogenase Assay. The *sqv-4*-coding sequences corresponding to the WT, *n2827*, and *n2840* alleles were cloned into the pET21d *Escherichia coli* expression vector and transformed into BL21 pLysS. All three proteins have a threonine-

Abbreviations: GAG, glycosaminoglycan; LG, linkage group; MBP, maltose-binding protein; Mel, maternal-effect lethal.

Data deposition: The sequence reported in this paper has been deposited in the GenBank database (accession no. AY147932).

*To whom correspondence should be addressed. E-mail: horvitz@mit.edu.

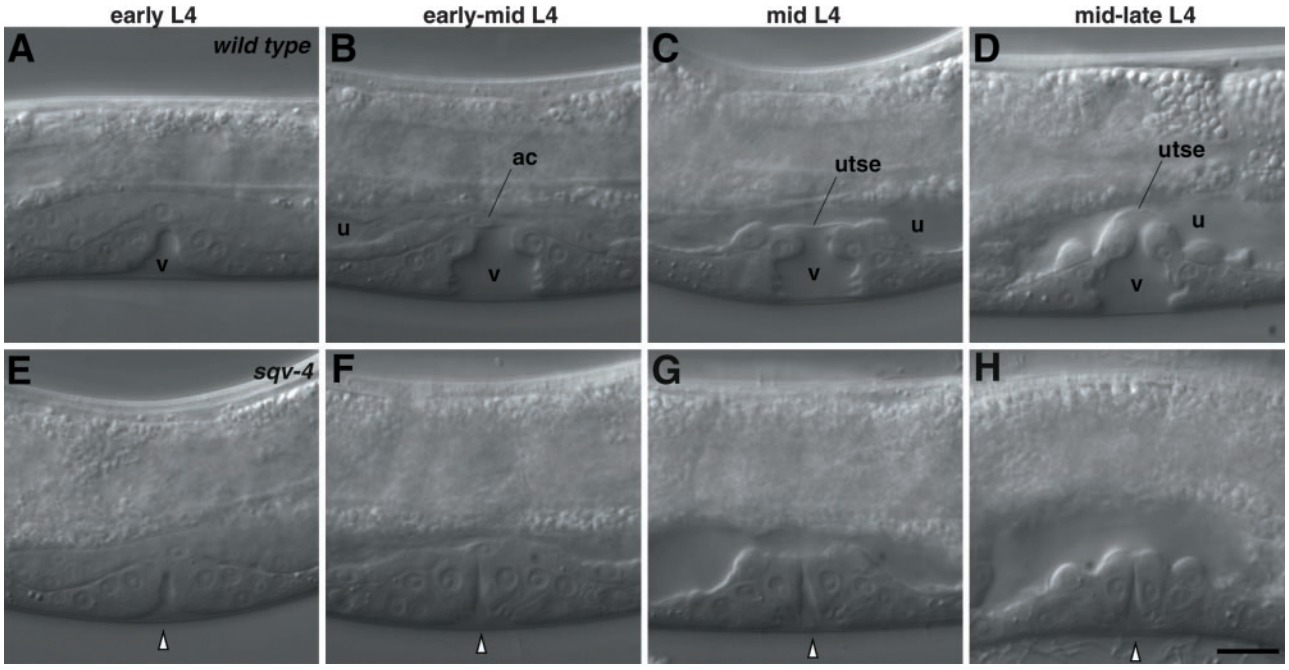

Fig. 1. Nomarski photomicrographs of vulval morphogenesis. Vulval morphogenesis in WT animals (*A–D*) and *sqv-4(n2827)* mutants (*E–H*) in sequential developmental stages. Anterior is on the left, and dorsal is up. (*A*) The vulval extracellular space (v) is a clear area devoid of granules. (*B*) The vulval extracellular space (v) is bottle-shaped. The uterine extracellular space (u) is a narrow area devoid of granules spanning the anterior to posterior ends and is separated from the vulval extracellular space by the anchor cell (ac). (*C*) The vulval (v) and uterine (u) extracellular spaces are separated by a thin planar cytoplasmic process of a uterine cell (utse). (*D*) A vulval extracellular space with an expanded dorsal end causing the utse cytoplasmic process to bend inward. *E–H* approximately correspond in developmental stage to the WT animals in *A–D*, respectively. The white arrowhead indicates the vulval extracellular space. (Scale bar = 10 μm.)

to-alanine mutation in the second amino acid because of the addition of an *Nco*I site at the 5′-end. SQV-4 expression was induced by incubation with 1 mM isopropyl β-D-thiogalactoside for 3–4 h at 37°C. *E. coli* were pelleted and resuspended in 50 mM Tris·HCl (pH 7.5), 1 mM DTT, 1 mM EDTA, 1 mM PMSF, and 2 μg/ml pepstatin A and aprotinin, and lysed using a French Pressure Cell. The soluble fraction was separated from the insoluble inclusion bodies by centrifugation at 12,000 $\times$ *g* for 20 min. Most of the recombinant SQV-4 protein was present in the soluble fraction, which was used for the UDP-glucose dehydrogenase assay without further purification.

UDP-glucose dehydrogenase activity was assayed spectrophotometrically by measuring the reduction of NAD^+ in the presence of UDP-glucose at 340 nm (19). All assays were performed at room temperature (≈22°C) in 50 mM Tris·HCl and 2 mM DTT (pH 8.7). Initial velocity was determined from time points during the first 60 s after addition of the SQV-4 extract. No reduction of NAD^+ was observed in the presence of 100 μM NAD^+ and 250 μM UDP-galactose, UDP-mannose, UDP-glucuronic acid, UDP-*N*-acetyl-glucosamine, ribosylthymine 5′-diphosphate-glucose, ADP-glucose, CDP-glucose, or GDP-glucose.

Abs and Immunostaining. The full-length *sqv-4*-coding sequence was cloned into vectors pGEX-4T3 and pMAL-c2 to generate GST-SQV-4 and maltose-binding protein (MBP)-SQV-4 fusion proteins, respectively. The GST-SQV-4 and MBP-SQV-4 fusion proteins were purified by isolating the insoluble fusion proteins in inclusion bodies followed by SDS/PAGE and electroelution. GST-SQV-4 was injected into two rabbits (Covance). Anti-SQV-4 antisera were affinity purified by binding to MBP-SQV-4 fusion protein bound to Optitran (Schleicher & Schuell) strips and eluting with 100 mM glycine, pH 2.5.

Whole worms were fixed by using a protocol based on Bouin's fixative (20). The fixed worms were incubated with anti-SQV-4 Abs and goat anti-rabbit FITC-conjugated secondary Abs (Jackson ImmunoResearch), as described by Finney and Ruvkun (21).

The staining patterns observed by whole-mount immunohistochemistry performed with Abs from both rabbits were indistinguishable at a gross level. Preimmune antisera showed staining comparable to that seen with the secondary Abs only (data not shown). Preabsorption of the Ab with GST-SQV-4 fusion protein reduced the whole-mount staining to background level (data not shown).

Expression of SQV-4-GFP from a *sqv-4* Promoter. An *Xma*I site was introduced immediately upstream of the stop codon of the *sqv-4* ORF. Using this *Xma*I site and a *Sal*I site upstream of the *sqv-4* ORF, a genomic fragment containing the *sqv-4* ORF and 6,253 bases upstream of the start codon of the *sqv-4* ORF was digested and ligated into the GFP vector pPD95.79 (from A. Fire). We injected *sqv-4(n2827)/nT1(n754)* animals with the *sqv-4* genomic locus and the 6,253 bases upstream of the predicted ATG transcriptionally fused to GFP in the vector pPD95.79. GFP-positive lines were established and were found to rescue *sqv-4*.

Results

Molecular Identification of *sqv-4*. *sqv-4* was previously mapped between *unc-42* and *sma-1* on LGV (10). We further mapped *sqv-4* between the left endpoint of *sDf35* and *emo-1* (Fig. 2*A*). Of the 13 cosmids we tested in this interval, two overlapping cosmids, C32C4 and C04G9, rescued *sqv-4* in germline transformation rescue experiments. A 4.8-kb *Eco*RV–*Xho*I fragment within the overlapping region between C32C4 and C04G9 containing a single gene, F29F11.1, was sufficient to rescue the *sqv-4* mutant phenotype.

We used the 4.8-kb minimal rescuing fragment as a probe to screen an embryonic cDNA library. One of the cDNAs obtained contained 1,443 bases of ORF, which is identical to F29F11.1 (Fig. 2*A*). Expression of the F29F11.1 ORF under the control of

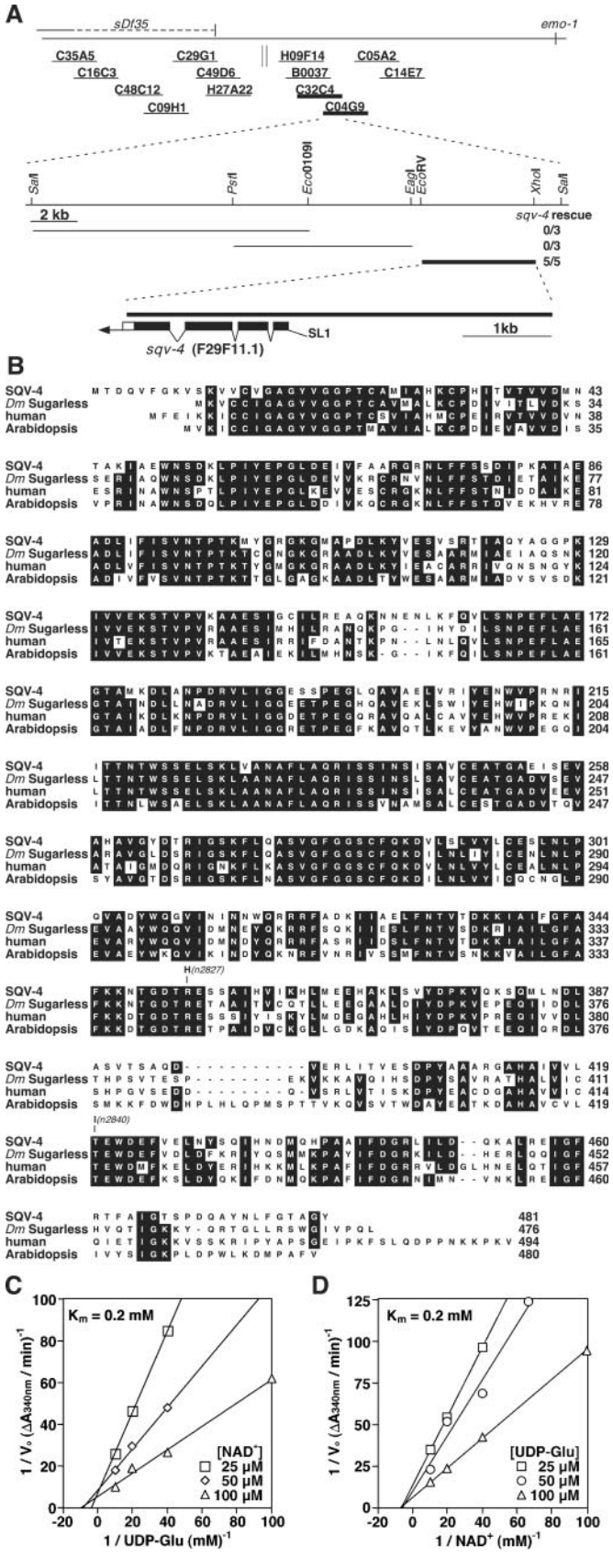

Fig. 2. *sqv-4* encodes a UDP-glucose dehydrogenase. (*A*) Cloning of *sqv-4*. (*Top*) Genetic and physical maps of the *sqv-4* locus. The dashed horizontal line depicting *sDf35* indicates the possible extent of the right end point of this deletion, which is between C35A5 and T21C9. Short solid horizontal lines represent cosmid clones that were assayed in germline transformation experiments. The parallel vertical lines indicate a gap in the cosmid coverage of the *C. elegans* genome. Cosmids that rescued the *sqv-4* mutant phenotype are shown in bold. (*Middle*) Subclones derived from the cosmids C32C4 or C04G9, corresponding to the common region shared by the two cosmids. Subclones that rescued the *sqv-4* mutant phenotype are shown in bold. The rescue experiment data are shown as the number of transformed lines that rescued/total. (*Bottom*) The structure of the *sqv-4* gene as deduced from the genomic and cDNA sequences. Solid boxes indicate exons, and open boxes indicate untranslated sequences. The trans-spliced leader SL1 is indicated, and the arrow indicates the poly(A) tail. (*B*) SQV-4 is similar to UDP-glucose dehydrogenases. UDP-glucose dehydrogenases of *Drosophila melanogaster* (*Sugarless*), human, and *Arabidopsis thaliana* are compared to SQV-4. The numbers on the right indicate amino acid positions. Identities among at least three proteins are shaded in black. The two *sqv*-4 missense alleles are indicated. (*C* and *D*) SQV-4 has UDP-glucose dehydrogenase activity. (*C*) A double-reciprocal plot of the initial reaction velocities with UDP-glucose as the variable substrate. Initial velocity was measured by using the linear phase of the reaction curve (intervals of 20–30 s). NAD^+ concentrations were 25 μM (□), 50 μM (◇), or 100 μM (△). (*D*) A double reciprocal plot of the initial reaction velocities with NAD^+ as the variable substrate. Initial velocity was measured by using the linear phase of the reaction curve (20- to 30-s intervals). UDP-glucose concentrations were 25 μM (□), 50 μM (○), or 100 μM (△). K_m values were calculated by the method of Lineweaver and Burke (39).

the *C. elegans* heat-shock promoters (18) rescued the vulval defect and the Mel defect of *sqv-4* mutants, indicating that the predicted coding sequence encodes a functional SQV-4 protein (data not shown). Specifically, heat-shock-induced expression of *sqv-4* from late embryogenesis through the second larval (L2) stage rescued the vulval but not the Mel defect conferred by *sqv-4* mutations. By contrast, heat-shock-induced expression of *sqv-4* in third or fourth stage (L3-L4) larvae or young adults successfully rescued the Mel defect. These data indicate *sqv-4* acts during at least two distinct phases of *C. elegans* development.

We identified molecular lesions in F29F11.1 in *sqv-4* mutants. Both mutant alleles, *n2827* and *n2840*, are missense mutations and are predicted to cause an arginine-to-histidine substitution at amino acid 353 and a threonine-to-isoleucine substitution at amino acid 420, respectively (Fig. 2*B*).

***sqv-4* Encodes a Protein Similar to UDP-Glucose Dehydrogenases.** The predicted SQV-4 protein is similar in amino acid sequence to a family of UDP-glucose dehydrogenases from vertebrates, insects, and plants (Fig. 2*B*). UDP-glucose dehydrogenase catalyzes the conversion of UDP-glucose to UDP-glucuronic acid (19, 22). Two molecules of NAD^+ are converted to NADH for each molecule of UDP-glucuronic acid that is generated (23). Of the 481 aa of SQV-4, 304 (63%), 303 (63%), and 272 (57%) are identical to the human, *Drosophila melanogaster*, and *Arabidopsis thaliana* UDP-glucose dehydrogenases, respectively. The two amino acids (R353 and T420) altered in the two *sqv-4* mutants are conserved among all known eukaryotic UDP-glucose dehydrogenases.

SQV-4 Has UDP-Glucose Dehydrogenase Activity. We tested recombinant SQV-4 protein expressed in *E. coli* for UDP-glucose dehydrogenase activity, which we assessed by monitoring the reduction of NAD^+ at 340 nm in the presence of UDP-glucose or other nucleotide sugars. We observed that UDP-glucose dehydrogenase activity was increased at least 20-fold in lysates containing SQV-4 protein compared to lysates containing mutant SQV-4 (R353H) protein, corresponding to the mutant allele *n2827* (data not shown).

We measured the initial velocities of this reaction varying either UDP-glucose or NAD^+. A double-reciprocal plot of the initial velocities revealed a K_m of 0.2 mM for UDP-glucose (Fig. 2*C*) and a K_m of 0.2 mM for NAD^+ (Fig. 2*D*). These K_m values

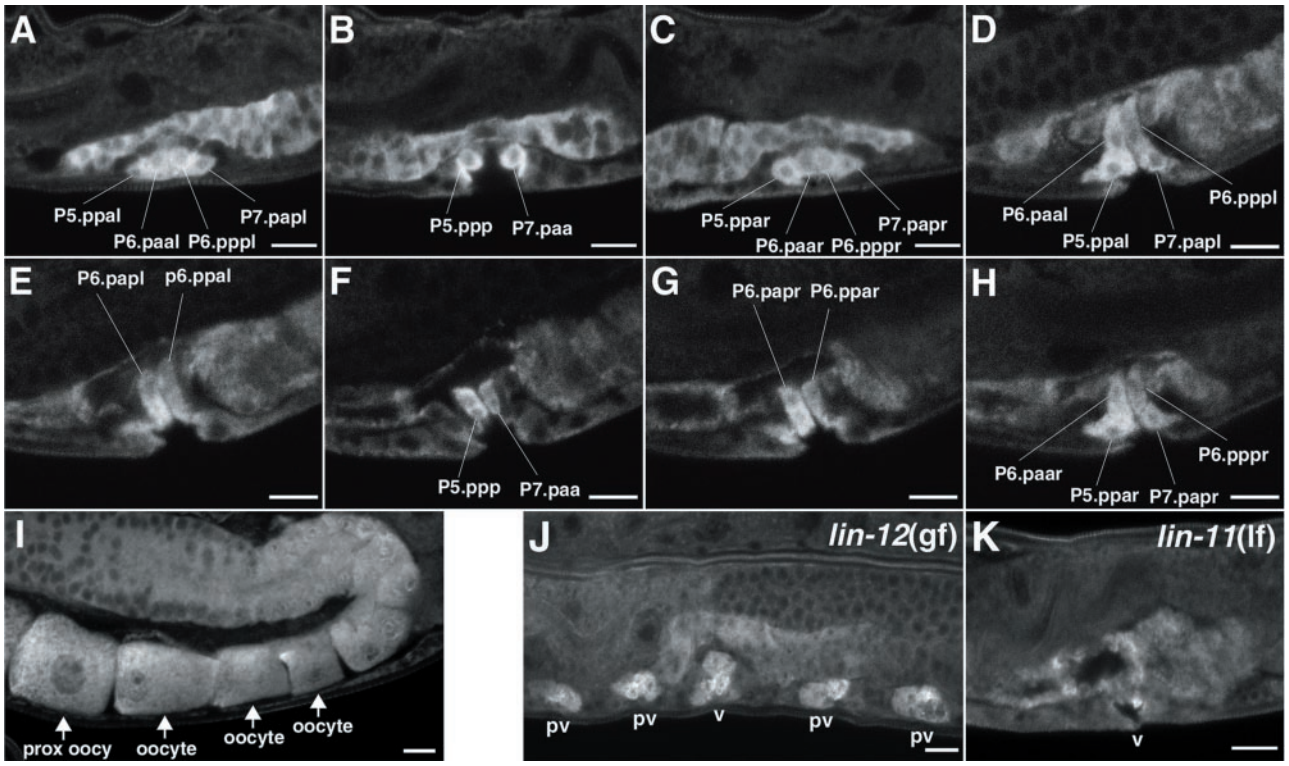

Fig. 3. SQV-4 protein expression. (*A–H*) Selected confocal images of SQV-4 Ab staining in multiple planes of focus along the left-to-right axis of the WT animal. Vulval cells with increased SQV-4 expression are indicated. (*A–C*) SQV-4 expression is increased in cells containing 10 of 22 vulval nuclei in the early L4 stage. The cells strongly stained with SQV-4 Abs dorsal to the vulval cells are in the uterus. The images are arranged from the left-most plane of focus to the right-most plane. (*A*) Vulval cells containing four nuclei (P5.ppal, P6.paal, P6.pppl, and P7.papl) on the left side of the worm. (*B*) Two vulval cells (P5.ppp and P7.paa) in the middle plane of the worm. (*C*) Vulval cells containing four nuclei (P5.ppar, P6.paar, P6.pppr, and P7.papr) on the right side of the worm. (*D–H*) SQV-4 expression is increased in cells containing 14 of 22 vulval nuclei in the mid-late L4 stage. The images are arranged from the left-most plane of focus to the right-most plane. (*D*) Vulval cells containing the same four nuclei as in *A*. (*E*) Vulval cells containing two of the four dorsal-most nuclei (P6.papl and P6.ppal), which were not stained at an earlier stage. (*F*) Vulval cells containing the same two nuclei as in *B*. (*G*) Vulval cells containing two of the four dorsal-most nuclei (P6.papr and P6.ppar), which were not stained at an earlier stage. (*H*) Vulval cells containing the same four nuclei as in *C*. (*I*) SQV-4 Abs stain oocytes. A row of oocytes in an adult hermaphrodite stained with SQV-4 Abs is indicated with arrows. The oocyte most proximal to the uterus is located at the lower left. (*J–K*) SQV-4 protein expression in mutants with abnormal vulval development. (*J*) Confocal image of a *lin-12*(gf) mutant fixed and stained with SQV-4 Abs. Each pseudovulva (pv) has three nuclei strongly stained with SQV-4 Abs. The functional vulva (v) has six nuclei strongly stained with SQV-4 Abs. Not all staining is shown here. (*K*) Confocal image of an L4 *lin-11*(lf) mutant fixed and stained with SQV-4 Abs. Staining by SQV-4 Abs is limited to one cell in this focal plane. Staining is absent in vulval cells in other focal planes (not shown). (Scale bar = 10 μm.)

are comparable to those of UDP-glucose dehydrogenases from other species; e.g., chicken has K_ms of 0.5 mM and 0.9 mM; *E. coli* has K_ms of 1 mM and 0.05 mM; and *Streptococcus pyogenes* has K_ms of 0.02 mM and 0.06 mM for UDP-glucose and NAD^+, respectively (24–26).

SQV-4 Protein Expression Is Dynamically Regulated in Vulval Cells During Vulval Morphogenesis. We raised rabbit polyclonal antisera against a GST-SQV-4 fusion protein and affinity-purified anti-SQV-4 Abs by using a MBP-SQV-4 fusion protein (see *Materials and Methods*). SQV-4 Abs stained the cytoplasm of many cells, including (but not limited to) oocytes and vulval cells, as well as uterine, seam, pharyngeal, and spermathecal cells (Fig. 3 *A–I*, data not shown). That SQV-4 is expressed in the developing vulva is consistent with its acting cell-autonomously in vulval morphogenesis. The presence of SQV-4 in oocytes is likely necessary for normal embryonic development.

In the WT, the vulva consists of the 22 descendants of the ventral hypodermal cells P5.p, P6.p, and P7.p. During the L3 larval stage, P5.p and P7.p divide to generate seven vulval descendants each, whereas P6.p divides to generate eight vulval descendants (27). During the L4 stage, the 22 vulval nuclei migrate inward and dorsally, with the inner nuclei of the P6.p descendants assuming the dorsal-most positions, and the outer nuclei of the P5.p and P7.p descendants assuming the ventral-most positions. The P5.p and the anterior half of the P6.p descendants become separated from the P7.p and the posterior half of the P6.p descendants by an expanding vulval extracellular space during the L4 stage (Fig. 1 *A–D*). This extracellular space initially expands so that the separation at the dorsal end is smaller than the separation at the ventral end (Fig. 1*A*). Then the middle of the vulval extracellular space widens (Fig. 1 *B* and *C*). Finally, the dorsal end of the vulval extracellular space expands toward the uterine cavity (Fig. 1*D*), and the vulval extracellular space collapses shortly thereafter (not shown). In *sqv-4* mutants, the expansion of the vulval invagination space is impaired (Fig. 1 *E–H*).

During the early L4 stage (see Fig. 1 *B* and *C*), 10 of the 22 vulval nuclei were in cells with dramatically increased expression of SQV-4 (Fig. 3 *A–C*). These 10 nuclei are the six inner nuclei of the P5.p and P7.p descendants and the four outer nuclei of the P6.p descendants (Fig. 4). During the mid-late L4 stage and thereafter (see Fig. 1*D*), cells containing the inner four nuclei of the P6.p descendants also increased SQV-4 expression, bringing the total of vulval nuclei that highly expressed SQV-4 to 14 (Fig. 3 *D–H*). Thus, the 22 vulval nuclei define three classes based on the levels and timing of SQV-4 expression (Fig. 4).

A transgene encoding SQV-4 tagged with GFP at its carboxyl

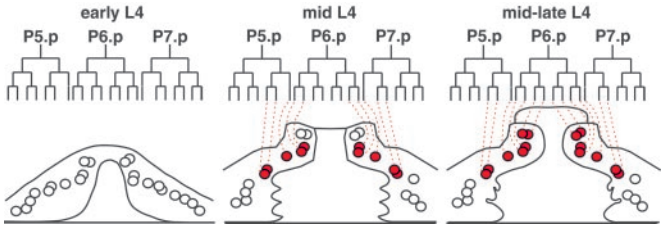

Fig. 4. Diagram of SQV-4 expression in vulval cells. WT vulval cell lineages and lateral views of vulva at three developmental stages. The vulva on the left, center, and right approximate the vulva in Fig. 1 *A*, *C*, and *D*, respectively. Circles indicate vulval cell nuclei, and overlapping circles indicate nuclei that are in different planes of focus along the left–right axis. Red circles, nuclei of the cells with increased SQV-4 expression. Open circles, nuclei of cells without detectable SQV-4 expression.

terminus and under the control of the endogenous *sqv-4* promoter was capable of rescuing the vulval and Mel defects of *sqv-4* mutants (data not shown). We observed GFP in many of the tissues stained by the SQV-4 Abs, including the vulva, uterus, intestine, seam, and hypodermis (data not shown). GFP was absent in oocytes, probably because expression from transgene arrays is silenced in the germline (28). GFP was observed in vulval cells containing 10 nuclei in the early L4 stage and in vulval cells containing 14 nuclei in later L4 (data not shown), consistent with the pattern of Ab staining.

The Number of SQV-4-Expressing Vulval Cells Is Increased in *lin-12*(gf) Mutants and Is Decreased in *lin-11*(lf) Mutants. In WT early L3 larvae, P5.p, P6.p, and P7.p form a row along the ventral side of the worm, with P3.p and P4.p to the anterior and P8.p to the posterior. P3.p, P4.p, and P8.p normally divide once to make two descendants that do not participate in vulva formation. In *lin-12* gain-of-function (gf) mutants, P3.p–P8.p all divide in P5.*p*- and P7.*p*-like patterns to generate seven descendants each, resulting in the formation of four pseudovulvae, each containing seven nuclei and one functional but abnormal vulva containing 14 nuclei (29). SQV-4 Abs strongly stained three nuclei of each pseudovulva and six nuclei of the functional vulva of *lin-12*(gf) mutant L4 stage larvae (Fig. 3*J*; data not shown). This result is consistent with the elevated expression of SQV-4 in three of the seven descendants of P5.p and P7.p in WT worms.

In *lin-11* loss-of-function (lf) mutants, P5.p and P7.p each generate eight vulval descendants. The *lin-11*(lf) P5.p and P7.p cell lineages are different from the WT P6.p cell lineage, which also generates eight descendants, in the orientation of the final cell division: The final WT P6.p divisions are along the left–right axis, whereas the final *lin-11* P5.p and P7.p divisions are along the anterior–posterior axis (30). *lin-11* mutants have an abnormally small vulval extracellular space, which is distinct from that of the *sqv* mutants, as only the ventral region is reduced in *lin-11* mutants. SQV-4 Abs strongly stained a smaller number of vulval cells in *lin-11* mutants compared to the WT, and SQV-4 staining in those vulval cells generally was also weaker (Fig. 3*K*; data not shown). An absence or reduced up-regulation of SQV-4 expression may be the cause of the smaller vulval extracellular space in *lin-11* mutants.

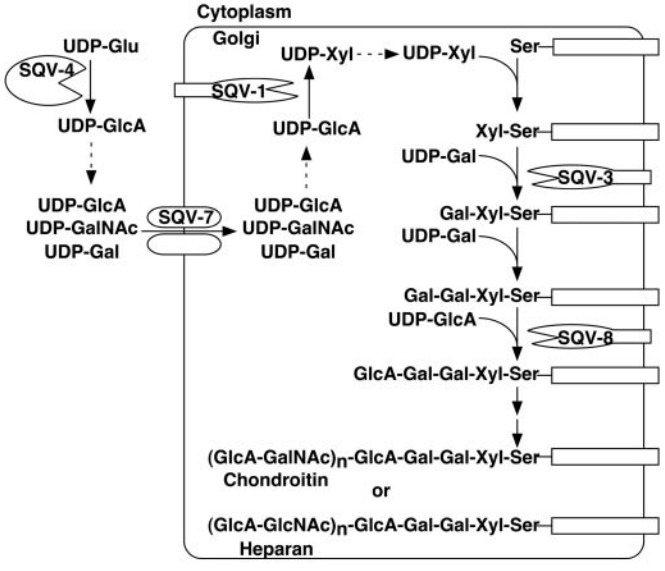

Fig. 5. Five SQV proteins function in GAG biosynthesis. SQV-4 converts UDP-glucose (UDP-Glu) to UDP-glucuronic acid (UDP-GlcA). SQV-7 transports UDP-GlcA, UDP-galactose (UDP-Gal), and UDP-*N*-acetylgalactosamine (UDP-GalNAc) from the cytoplasm to the Golgi apparatus (3). SQV-1 converts UDP-GlcA to UDP-xylose (UDP-Xyl). SQV-3 is galactosyltransferase I, which uses UDP-Gal as the donor sugar (2). SQV-8 is glucuronyltransferase I, which uses UDP-GlcA as the donor sugar (2). Two additional set of glycosyltransferases act in the biosynthesis of chondroitin and heparan sulfate GAGs. UDP-glucuronic acid is required for biosynthesis of both GAGs. The two GAGs differ by the composition of the amino sugar in the repeating disaccharide region: Chondroitin has *N*-acetylgalactosamine (GalNAc), and heparan has *N*-acetylglucosamine (GlcNAc) assembled by using their UDP-derivatives as substrates.

Discussion

sqv-4 encodes a UDP-glucose dehydrogenase that converts UDP-glucose to UDP-glucuronic acid, which is a necessary substrate for the biosynthesis of chondroitin and heparan sulfate GAGs. Both chondroitin and heparan sulfate GAGs use glucuronic acid as one of the two sugars in the repeating disaccharide domain: *N*-acetylglucosamine and *N*-acetylgalactosamine are the second sugar for heparan and chondroitin GAGs, respectively (reviewed in ref. 9). The levels of chondroitin and heparan sulfate GAGs are reduced in *sqv-3*, *-7*, and *-8* mutants (2). UDP-glucuronic acid is important in the biochemical functions of SQV-1, SQV-7, and SQV-8. SQV-7 translocates UDP-glucuronic acid across the Golgi membranes (3). SQV-1 converts UDP-glucuronic acid to UDP-xylose (4). SQV-8 uses a UDP-glucuronic acid donor to catalyze its glycosylation reaction (1, 2). We propose that like *sqv-1*, *-3*, *-7*, and *-8*, *sqv-4* also acts in the biosynthesis of GAGs and is the earliest gene in the biosynthetic pathway for GAGs among the five cloned *sqv* genes (Fig. 5). We suspect that a complete loss of *sqv-4* gene function would cause a phenotype identical to that of the missense mutants, but we cannot preclude the possibility that a *sqv-4* null mutant is haploinsufficient for embryonic and larval development.

In addition to being required for GAG biosynthesis, SQV-4 may also participate in other biochemical pathways. In mammals, UDP-glucuronic acid is a necessary substrate for the biosynthesis of hyaluronan (reviewed in refs. 31 and 32). The presence in *C. elegans* of heparan sulfate and unsulfated chondroitin has been reported, but hyaluronan is apparently absent (33). UDP-glucuronic acid is also used for the formation of certain *N*- and *O*-glycans in mammals, notably the HNK-1 epitope, which contains a terminal sulfated glucuronic acid (34). However, we have failed to detect the presence of the HNK-1 epitope in *C. elegans* (H.-Y.H. and H.R.H., unpublished observations) by using anti-HNK-1 Abs (35). Finally, UDP-glucuronic acid may be used as a substrate by a large family of proteins similar to liver glucuronyltransferases involved in the detoxification of potentially harmful chemicals in the digestive tract; the *C. elegans* genome contains 69 potential such glucuronyltransferases (36). Perhaps *sqv-4* is important for detoxifying harmful chemicals in *C. elegans* in its natural environment. In support of the hypothesis that SQV-4 has multiple roles, we have found that SQV-4 is

expressed in many cell types, including the vulva, uterus, oocyte, and seam. However, because *sqv-4* mutants display the same vulval mutant phenoytpe as seen in *sqv-1*, *-3*, *-7*, and *-8* mutants, we suggest that the vulval defects are caused by deficiencies in GAG biosynthesis.

The increased expression of SQV-4 in a specific subset of L4-stage vulval cells may indicate that an increased level of UDP-glucuronic acid in those vulval cells leads to an increase in the amount and lengths of chondroitin and heparan sulfate GAGs. The regulation of chondroitin and/or heparan sulfate proteoglycan biosynthesis in those cells may in turn control an aspect of vulval morphogenesis. The temporal and spatial increase of SQV-4 expression in a subset of the vulval cells parallels the stereotypical changes in the shape of the vulval extracellular space during the L4 stage. For example, the widening of the middle of the vulval extracellular space coincides with the increased SQV-4 expression in the cells containing 10 vulval nuclei located in the center of the dorso-ventral axis. Similarly, the final expansion of the dorsal end of the extracellular space coincides with the increased expression of SQV-4 in the cells containing the four dorsal-most vulval nuclei.

Unlike the SQV-4 protein, the SQV-1, SQV-5, and SQV-7 proteins are expressed constitutively in all vulval cells (ref. 4; H.-Y.H. and H.R.H., unpublished observations), suggesting that the temporal and spatial regulation of *sqv-4* may be unique among *sqv* genes. Perhaps most of the SQV proteins involved in GAG biosynthesis are constitutively present, whereas one or a few, including SQV-4, act as control points for the rapid synthesis of GAGs. SQV-4 seems to be a plausible control point because the conversion of UDP-glucose to UDP-glucuronic acid is irreversible and the absence of SQV-4 may conserve UDP-glucose (and glucose) in the cell. We have not observed any striking abnormalities associated with overexpression of *sqv-4* (data not shown). For this reason, we postulate that although *sqv-4* regulation is likely to be important, the regulation of at least one other gene (perhaps the gene that encodes the protein core for this glycosylation process) is at least equally important.

What is the protein core of the chondroitin and/or heparan sulfate that acts in vulval morphogenesis and/or embryonic development, and how does the protein core control the changes in the vulval extracellular matrix? In the accompanying paper (4), we discuss the possibility of GAGs affecting osmotic pressure, adhesion, and intercellular signaling. Heparan sulfate GAGs in *Drosophila* and zebrafish have been proposed to interact with signaling molecules in part because the developmental abnormalities of mutants defective in the biosynthesis of GAGs and signaling molecules are similar (37, 38). No *C. elegans* mutant defective in a signaling pathway has been found that exhibits a Sqv phenotype. A protein core might be encoded by one of the as yet uncloned *sqv* genes. On the other hand, it is possible that multiple different proteoglycan protein cores are involved in vulval morphogenesis. If so, the genes that encode these proteins may function redundantly and may not be included in the current set of *sqv* genes identified by their nonredundant roles in vulval morphogenesis (10).

We thank Beth Castor for help with DNA sequencing; the laboratory of Tim Schedl for providing a strain containing the *emo-1(oz1)* mutation; Andy Fire for GFP and heat-shock vectors; and Alan Coulson and the *C. elegans* Sequencing Consortium for cosmid DNA clones. We also thank Peter Reddien, Ewa Davison, and Niels Ringstad for critical reading of this manuscript. This work was supported by National Institutes of Health Grant GM24663. H.R.H. is an Investigator of the Howard Hughes Medical Institute.

1. Herman, T. & Horvitz, H. R. (1999) *Proc. Natl. Acad. Sci. USA* **96,** 974–979.
2. Bulik, D. A., Wei, G., Toyoda, H., Kinoshita-Toyoda, A., Waldrip, W. R., Esko, J. D., Robbins, P. W. & Selleck, S. B. (2000) *Proc. Natl. Acad. Sci. USA* **97,** 10838–10843.
3. Berninsone, P., Hwang, H. Y., Zemtseva, I., Horvitz, H. R. & Hirschberg, C. B. (2001) *Proc. Natl. Acad. Sci. USA* **98,** 3738–3743.
4. Hwang, H.-Y. & Horvitz, H. R. (2002) *Proc. Natl. Acad. Sci. USA* **99,** 14218–14223.
5. Okajima, T., Yoshida, K., Kondo, T. & Furukawa, K. (1999) *J. Biol. Chem.* **274,** 22915–22918.
6. Almeida, R., Levery, S. B., Mandel, U., Kresse, H., Schwientek, T., Bennett, E. P. & Clausen, H. (1999) *J. Biol. Chem.* **274,** 26165–26171.
7. Okajima, T., Fukumoto, S., Furukawa, K. & Urano, T. (1999) *J. Biol. Chem.* **274,** 28841–28844.
8. Duncan, G., McCormick, C. & Tufaro, F. (2001) *J. Clin. Invest.* **108,** 511–516.
9. Kjellen, L. & Lindahl, U. (1991) *Annu. Rev. Biochem.* **60,** 443–475.
10. Herman, T., Hartwieg, E. & Horvitz, H. R. (1999) *Proc. Natl. Acad. Sci. USA* **96,** 968–973.
11. Brenner, S. (1974) *Genetics* **77,** 71–94.
12. Riddle, D. L., Blumenthal, T., Meyer, B. J. & Priess, J. R. (1997) *C. elegans II* (Cold Spring Harbor Lab. Press, Plainview, NY).
13. McKim, K. S., Heschl, M. F., Rosenbluth, R. E. & Baillie, D. L. (1988) *Genetics* **118,** 49–59.
14. Ferguson, E. L. & Horvitz, H. R. (1985) *Genetics* **110,** 17–72.
15. Sambrook, J., Fritsch, E. F. & Maniatis, T. (1989) *Molecular Cloning: A Laboratory Manual* (Cold Spring Harbor Lab. Press, Plainview, NY).
16. Mello, C. C., Kramer, J. M., Stinchcomb, D. & Ambros, V. (1991) *EMBO J.* **10,** 3959–3970.
17. Okkema, P. G. & Fire, A. (1994) *Development (Cambridge, U.K.)* **120,** 2175–2186.
18. Stringham, E. G., Dixon, D. K., Jones, D. & Candido, E. P. (1992) *Mol. Biol. Cell* **3,** 221–233.
19. Strominger, J. L., Kalckar, H. M., Axelrod, J. & Maxwell, E. S. (1954) *J. Am. Chem. Soc.* **76,** 6411–6412.
20. Nonet, M. L., Staunton, J. E., Kilgard, M. P., Fergestad, T., Hartwieg, E., Horvitz, H. R., Jorgensen, E. M. & Meyer, B. J. (1997) *J. Neurosci.* **17,** 8061–8073.
21. Finney, M. & Ruvkun, G. (1990) *Cell* **63,** 895–905.
22. Hempel, J., Perozich, J., Romovacek, H., Hinich, A., Kuo, I. & Feingold, D. S. (1994) *Protein Sci.* **3,** 1074–1080.
23. Strominger, J. L., Maxwell, E. S., Axelrod, J. & Kalckar, H. M. (1956) *J. Biol. Chem.* **224,** 79–90.
24. Bdolah, A. & Feingold, D. S. (1968) *Biochim. Biophys. Acta* **159,** 176–178.
25. Schiller, J. G., Bowser, A. M. & Feingold, D. S. (1973) *Biochim. Biophys. Acta* **293,** 1–10.
26. Campbell, R. E., Sala, R. F., van de Rijn, I. & Tanner, M. E. (1997) *J. Biol. Chem.* **272,** 3416–3422.
27. Sulston, J. E. & Horvitz, H. R. (1977) *Dev. Biol.* **56,** 110–156.
28. Kelly, W. G., Xu, S., Montgomery, M. K. & Fire, A. (1997) *Genetics* **146,** 227–238.
29. Greenwald, I. S., Sternberg, P. W. & Horvitz, H. R. (1983) *Cell* **34,** 435–444.
30. Freyd, G., Kim, S. K. & Horvitz, H. R. (1990) *Nature* **344,** 876–879.
31. Lindahl, U. & Hook, M. (1978) *Annu. Rev. Biochem.* **47,** 385–417.
32. Terayama, K., Oka, S., Seiki, T., Miki, Y., Nakamura, A., Kozutsumi, Y., Takio, K. & Kawasaki, T. (1997) *Proc. Natl. Acad. Sci. USA* **94,** 6093–6098.
33. Yamada, S., Van Die, I., Van den Eijnden, D. H., Yokota, A., Kitagawa, H. & Sugahara, K. (1999) *FEBS Lett.* **459,** 327–331.
34. Voshol, H., van Zuylen, C. W., Orberger, G., Vliegenthart, J. F. & Schachner, M. (1996) *J. Biol. Chem.* **271,** 22957–22960.
35. Abo, T. & Balch, C. M. (1981) *J. Immunol.* **127,** 1024–1029.
36. *C. elegans* Sequencing Consortium (1998) *Science* **282,** 2012–2018.
37. Walsh, E. C. & Stainier, D. Y. (2001) *Science* **293,** 1670–1673.
38. Perrimon, N. & Bernfield, M. (2000) *Nature* **404,** 725–728.
39. Lineweaver, H. & Burk, D. J. (1934) *J. Am. Chem. Soc.* **56,** 658–666.